

Using Deep Ensemble Forest for High Resolution Mapping of PM_{2.5} from MODIS MAIAC AOD in Tehran, Iran

Hossein Bagheri

Faculty of Civil Engineering and Transportation, University of Isfahan, Azadi square, Isfahan, 8174673441, Iran.

Corresponding author(s). E-mail(s): h.bagheri@cet.ui.ac.ir;

Abstract

This is the pre-acceptance version, to read the final version, please go to Environmental Monitoring and Assessment on Springer, URL: <https://rdcu.be/c5ipl>. High resolution mapping of PM_{2.5} concentration over Tehran city is challenging because of the complicated behavior of numerous sources of pollution and the insufficient number of ground air quality monitoring stations. Alternatively, high resolution satellite Aerosol Optical Depth (AOD) data can be employed for high resolution mapping of PM_{2.5}. For this purpose, different data-driven methods have been used in the literature. Recently, deep learning methods have demonstrated their ability to estimate PM_{2.5} from AOD data. However, these methods have several weaknesses in solving the problem of estimating PM_{2.5} from satellite AOD data. In this paper, the potential of the deep ensemble forest method for estimating the PM_{2.5} concentration from AOD data was evaluated. The results showed that the deep ensemble forest method with $R^2 = 0.74$ gives a higher accuracy of PM_{2.5} estimation than deep learning methods ($R^2 = 0.67$) as well as classic data-driven methods such as random forest ($R^2 = 0.68$). Additionally, the estimated values of PM_{2.5} using the deep ensemble forest algorithm were used along with ground data to generate a high resolution map of PM_{2.5}. Evaluation of produced PM_{2.5} map revealed the good performance of the deep ensemble forest for modeling the variation of PM_{2.5} in the city of Tehran.

Keywords: Air pollution, PM_{2.5} measurements, AOD measurements, Deep ensemble forest, Deep learning, Deep model, Ensemble learning, Decision trees

1 Introduction

Particulate matter (PM) is one of the main reasons for various diseases and mortality, particularly in industrialized and urban areas. Urbanization has increased the level of PM in recent decades and has caused severe health problems, which is one of the hot topics of environmental investigations and health studies. Studies illustrate particulate matters with sizes less than 2.5, called PM_{2.5}, is the most harmful and dangerous pollutant exposing populations living in polluted areas such as metropolitan and industrialized areas [Klemm, Mason Jr, Heilig, Neas, and Dockery \(2000\)](#); [Lippmann, Ito, Nadas, and Burnett \(2000\)](#). Consequently, monitoring the level of PM_{2.5} is a crucial and significant task for health surveillance and epidemiological studies.

Conventionally, PM_{2.5} concentration is measured using a network of air quality monitoring stations located in residential areas. The in-situ measurements are used to determine the air quality index of the covered area. Due to few monitoring stations, the level of pollutants cannot be estimated accurately in the interspaces of monitoring stations.

One of the main useful sources that can compensate for the lack of in-situ measurements is data collected by satellites which provide high resolution measurements with extensive coverage. Satellite sensors measure levels of pollutant particles (namely aerosol) in a column from the ground surface toward the sensor at the top of the atmosphere. In other words, the AOD product shows the amount of aerosols in the atmosphere. A higher value of AOD means a higher amount of aerosols in the atmosphere. Several satellite sensors such as Aqua and Terra have been designed to measure AOD. Both of the aforementioned sensors are mounted on the Moderate Resolution Imaging Spectroradiometer (MODIS) satellite, which has provided the possibility of daily measurement of aerosol particles in a wide area. The observations collected by Aqua and Terra sensors are converted into AOD data using different algorithms. Dark Target (DT) and Deep Blue (DB) algorithms are two well-known algorithms for AOD retrieval from satellite observations such as those acquired by Aqua and Terra. The DT algorithm is mostly used to retrieve AOD in areas with high vegetation density, which reduces its efficiency in urban areas (areas with a lack of dense vegetation). In contrast, DB is designed to retrieve AOD on bright surfaces in urban areas [Hsu et al. \(2013\)](#); [Sayer, Hsu, Bettenhausen, Jeong, and Meister \(2015\)](#). However, both algorithms lead to AOD products with a resolution of 10 or 3 *km*, which are not desirable to monitor the variation of PM_{2.5} concentration in urban areas. Recently, the Multi-Angle Implementation of Atmospheric Correction (MAIAC) algorithm has been developed to retrieve AOD data from satellite observations, which has provided an opportunity to estimate AOD at a higher resolution (1 *km*) [Lyapustin, Zhao, and Wang \(2021\)](#). Several studies have demonstrated the potential of MAIAC AOD data for high resolution estimation of PM_{2.5} concentration [Di et al. \(2016\)](#); [Xiao et al. \(2017\)](#). In order to retrieve AOD, this algorithm uses consecutive observations (time series) of Aqua and Terra sensors in a short period. As a result,

it is possible to separate the reflection caused by dynamic phenomena such as aerosol and cloud versus the reflection caused by static surface phenomena.

The AOD data retrieved from satellite measurements can be potentially used for PM_{2.5} estimation [J. Wang and Christopher \(2003a\)](#). However, PM_{2.5} is a surface measurement, while AOD represents the content of aerosol in a column from the near-earth surface toward the sensor. Consequently, estimating the PM_{2.5} level from AOD is a challenging task. Different techniques have been applied for modeling and estimating PM_{2.5} from satellite AOD measurements which lie in three main categories: chemical simulations, statistical modeling, and semi-empirical modeling [Lin et al. \(2015\)](#); [Song, Jia, Huang, and Zhang \(2014\)](#); [Van Donkelaar et al. \(2010\)](#). Among these modeling techniques, statistical approaches are mainly based on data-driven methods (also called machine learning methods) and have been widely applied for modeling the AOD-PM_{2.5} relationship [Gupta and Christopher \(2009b\)](#); [Y. Liu et al. \(2004\)](#); [Ma et al. \(2016\)](#); [Yao, Si, Li, and Wu \(2018\)](#). In this regard, different machine learning techniques have been employed to estimate PM_{2.5} concentration [Ahmad et al. \(2019\)](#); [W. Chen et al. \(2020\)](#); [Gupta and Christopher \(2009a, 2009c\)](#); [T. Li, Shen, Yuan, Zhang, and Zhang \(2017\)](#); [Ni, Cao, Zhou, Cui, and P. Singh \(2018\)](#); [Sun, Gong, and Zhou \(2021\)](#); [Weizhen et al. \(2014\)](#).

Indeed, estimating PM_{2.5} from AOD measurements is considered a regression problem, and machine learning-based regression techniques try to explore a model based on the AOD variable as input and PM_{2.5} as output. The basic approach relies on a univariate regression model. Wang and Christopher showed a meaningful correlation between AOD and PM_{2.5} [J. Wang and Christopher \(2003a\)](#). However, the univariate model does not always have acceptable performance in constructing the relationship between those variables. The main reason is the complex behaviors of aerosols that are mostly affected by atmospheric conditions. Thus, some studies proposed to involve meteorological parameters such as boundary layer height, relative humidity, surface pressure, air temperature, etc., for modeling the relationship between PM_{2.5} and AOD [Arciszewska and McClatchey \(2001\)](#); [Gupta and Christopher \(2009b\)](#). Including more parameters in PM_{2.5} estimation from AOD demands the development of more efficient regression models. For this purpose, the univariate model was upgraded to a multivariate model [Gupta and Christopher \(2009b\)](#). In addition, several studies suggested more advanced models with the ability to employ more input features and explore sophisticated patterns [T. Li et al. \(2017\)](#); [Sun et al. \(2021\)](#).

For PM_{2.5} estimation using AOD data, neural networks, a type of popular machine learning technology, have been used in several studies [Gupta and Christopher \(2009a\)](#); [Ni et al. \(2018\)](#). Deep neural networks have demonstrated excellent performance in a variety of machine learning problems in recent years. Deep learning algorithms have also been used to estimate PM_{2.5} from satellite data and compared to decision tree ensemble methodologies. Several studies have demonstrated the superiority of deep learning over traditional machine

learning models [L. Li \(2020\)](#); [X. Wang and Sun \(2019\)](#). Li et al. designed a geointelligent network for PM_{2.5} estimate utilizing satellite AOD measurements based on deep belief networks [T. Li et al. \(2017\)](#). For predicting PM_{2.5} and PM₁₀ from AODs, Li employed autoencoder-based residual networks [L. Li \(2020\)](#). The PM_{2.5}-AOD modeling was discovered by Chen et al. using a self-adaptive deep neural network [B. Chen et al. \(2021\)](#).

In general, deep neural networks suffer from some deficiencies such as having too many hyperparameters, demanding many training data, and requiring powerful computational facilities. Exploring patterns in sophisticated regression problems requires increasing complexity of network structure, i.e. adding more hidden layers. However, adding more layers makes the structure uninterpretable (black box). Moreover, increasing the network's capacity for providing sufficient complexity of the model will raise the probability of overfitting. On the other hand, training a deeper network is trickier and more complicated than a shallow neural network. Additionally, deep neural networks rely on weight optimization by backpropagation of errors. Backpropagation requires more computational loads and gradients could be exploded or vanished during training.

Regarding the advantages and defects of deep neural networks, a recent development was established to devise a deep model such as a deep neural network but with non-differentiable modules (without backpropagation). For this, an ensemble approach based on decision trees estimators such as random forest, extremely randomized trees, etc., so-called deep ensemble forest, was developed. It takes the useful characteristics of deep neural networks such as layer-by-layer processing, in-model feature transformation, and sufficient model complexity while does not need any backpropagation process. In this way, the advantages of decision tree ensemble approaches and deep neural networks are combined in dealing with complex regression problems [Zhou and Feng \(2017\)](#). [Lyapustin et al. \(2021\)](#); ? Considering the aforementioned properties of deep ensemble forest, the main objective of this paper is to assess the potential of deep ensemble forest for estimating PM_{2.5} concentration from MODIS AOD (1 km MAIAC), weather data, and PM_{2.5} observations collected at air quality monitoring stations over Tehran city. The PM_{2.5} calculation using AOD data was performed in the research area using the 3 or 10 km (DB or DT) products provided by MODIS. In a brief time of observations, Sotoudeheian and Arhami calculated PM_{2.5} using 10 km DT AODs. The correlation between anticipated and observed PM_{2.5} levels was around 0.55 [Sotoudeheian and Arhami \(2014\)](#). Ghotbi et al. used 3 km DT AOD and limited samples gathered from few ground stations for a very short time to estimate PM_{2.5} over Tehran with higher accuracy ($R^2 = 0.73$) [Ghotbi, Sotoudeheian, and Arhami \(2016\)](#). Another study used the 10 km MODIS AOD retrievals to estimate PM_{2.5} over Tehran. The achievements showed that machine learning improved accuracy by up to 80% [Zamani Joharestani, Cao, Ni, Bashir, and Talebiesfandarani \(2019\)](#). A further study in Tehran utilizing MAIAC AOD data for PM_{2.5} estimation found a correlation of smaller than 0.5, [Nabavi, Haimberger,](#)

and Abbasi (2019), which is not ideal for high resolution AOD-based PM_{2.5} mapping. In a recent study, a map of PM_{2.5} at 1 km resolution over the city was realized from MAIAC AOD products using a machine learning framework Bagheri (2022).

As mentioned earlier, no study in the literature has focused on the capability of deep ensemble forest in comparison to deep neural networks for PM_{2.5} estimation from AOD data. Thus this paper also investigates the performance of deep ensemble forest in comparison to some common deep neural networks structures implemented in previous studies such as deep belief networks and deep autoencoders L. Li (2020); T. Li et al. (2017). In addition, the accuracy of deep ensemble forest in estimating PM_{2.5} is also compared with other advanced machine learning algorithms such as random forest, and extra trees, etc. that can outperform deep models in regression problems, particularly when dealing with tabular data and measurements.

This paper consists of seven sections. The introduction, the literature review, and the objectives of the paper were explained earlier in this section. The study area and datasets used in this investigation will be introduced in Section 2. The description of the deep ensemble forest algorithm is provided in Section 3. The implementation of deep ensemble forest for high resolution estimation of PM_{2.5} is realized through a framework including different stages, preprocessing of input materials; regression; and deployment which will be explained in Section 4. Section 4 also provides experimental setups that were used for tuning and training the deep ensemble forest and other machine learning techniques. The results of deep ensemble forest regression are compared with other machine learning and deep learning techniques in the following (Section 5). Section 5.2 discusses the performance of deep ensemble forest for 1 km estimation of PM_{2.5} as daily and annual PM_{2.5} maps over Tehran. Finally, a conclusion of the investigation is presented in Section 6.

2 Study Area and Datasets

The study region in this research is Tehran, Iran's capital, as a metropolitan residential area with a population of more than 16 million people. It is located at an area spread from latitude 35° 35' N to 35°48' N and longitude 51°17' E to 51° 33' E. Elevations change between 900 m and 1800 m higher than the mean sea level. Tehran suffers from air pollution, particularly in the winter season, induced from different sources such as pollution emitted from mobile vehicles and emissions from manufactures located in the suburb. Fig. 1 displays the limit of Tehran city as well as locations of air quality stations. In-situ measurements are collected by these stations, which will be described more in the following.

2.1 PM_{2.5} In-situ Measurements

As shown in Fig. 1, 23 air quality monitoring stations scattered across Tehran urban area have been launched by the Air Quality Control Company (AQCC):

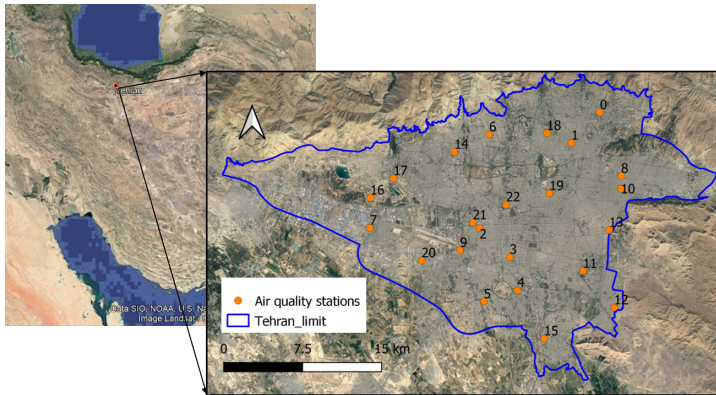


Fig. 1 A display of the study area. Numbers have been assigned by the author for further analysis in Section 5.

<http://airnow.tehran.ir/home/DataArchive.aspx>) of Tehran. PM_{2.5} is measured hourly at each station. However, measurements in some stations are missed occasionally due to technical problems. The daily PM_{2.5} is achieved by averaging hourly observations. In this study, daily measurements from Jan. 2013 to Dec. 2019 (7 years) were collected to model the PM_{2.5} variation.

2.2 Satellite AOD Measurements

Several types of AOD products are retrieved from observations by spaceborne sensors J. Wang and Christopher (2003b); Yao et al. (2018); You, Zang, Pan, Zhang, and Chen (2015). A famous product is the Multiangle Implementation of Atmospheric Correction (MAIAC) AOD, which is produced at 1 km resolution from measurements generated by Aqua and Terra sensors on the MODIS platform. The MAIAC algorithm for AOD retrieval is achieved by time series processing of satellite observations, which allows dynamic phenomena like aerosols and clouds to be separated from static surface features. Lyapustin, Wang, Korkin, and Huang (2018). In this study, daily AOD products were generated from initial MAIAC AOD retrievals during the study period. The MODIS Version 6 MAIAC AOD data (MCD19A2.006) were achieved in HDF format from the EarthData portal of NASA (<https://search.earthdata.nasa.gov/search>). Finally, the AOD at each monitoring station was extracted by a 3×3 window from daily MAIAC grids. More details will be provided in Section 4.1.

2.3 Meteorological Data

Alongside the satellite AOD, meteorological data also have significant roles in PM_{2.5} estimation Arciszewska and McClatchey (2001); Gupta and Christopher (2009a, 2009c); Ni et al. (2018). For example, boundary layer height has a vital role in distinguishing the surface PM_{2.5} level from total columnar aerosols Gupta and Christopher (2009b). In this study, different meteorological

parameters such as temperature (T), dewpoint temperature (DT), planetary boundary layer height (PBLH), surface pressure (SP), wind properties (WS, WD), leaf area index (LAI), UV radiation (UV), and relative humidity (RH) were employed for PM_{2.5}-AOD modeling. The meteorological data were derived from the ERA5 weather model that is developed by European Centre for Medium-Range Weather Forecasts (ECMWF) [ECMWF \(2021\)](#); [Hersbach et al. \(2020\)](#). The employed data can be achieved in NetCDF format from Copernicus Climate Data Store (<https://cds.climate.copernicus.eu/>).

In addition to the aforementioned features, other parameters such as positional data, i.e., latitude (Lat), and longitude (Long), and day of year (DOY) as a time variable were involved for final estimation. The statistical summaries, and detailed descriptions of input features applied for PM_{2.5} modeling using satellite AOD have been collected in Tab. 1.

Table 1 List of input parameters employed for PM_{2.5} estimation in Tehran

Feature	Description	Max	Mean	Min	Std
AOD	Aerosol optical depth	0.88	0.17	0.01	0.08
U	AOD Uncertainty	1	0.41	0	0.24
PM	PM _{2.5}	64.80	28.99	0.60	12.02
Lat	Latitude	35.80	35.71	35.60	0.05
Long	Longitude	51.51	51.38	51.24	0.08
T	2m temperature	308.44	289.56	262.39	10.52
DT	2m dewpoint temperature	286.54	271.87	250.52	5.22
PBLH	Planetary boundary layer height	1981.97	702.30	27.75	382.16
SP	Surface pressure	2.33	1.81	1.30	0.27
LAI	Leaf area index	0.53	0.50	0.47	0.01
WS	10m wind speed	4.91	1.81	0.70	0.47
WD	10m wind direction	2.44	-0.44	-2.31	0.61
UV	UV radiation	139511.69	100547.60	33686.45	28484.86
RH	Relative humidity	0.94	0.69	0.41	0.12
DOY	Day of year	365	185.69	1	96.42

3 Methods

The main purpose of this study is to build a model (F) that can predict concentration of PM_{2.5} from input features, AOD; meteorological information; and other auxiliary data as below:

$$PM = F(AOD, U, Lat, Long, T, DT, PBLH, SP, LAI, WS, WD, UV, RH, DOY), \quad (1)$$

where F is a functional model that associates AOD and other input features to PM_{2.5}. The descriptions of other notations have been provided in Section 2.3 and Tab. 1.

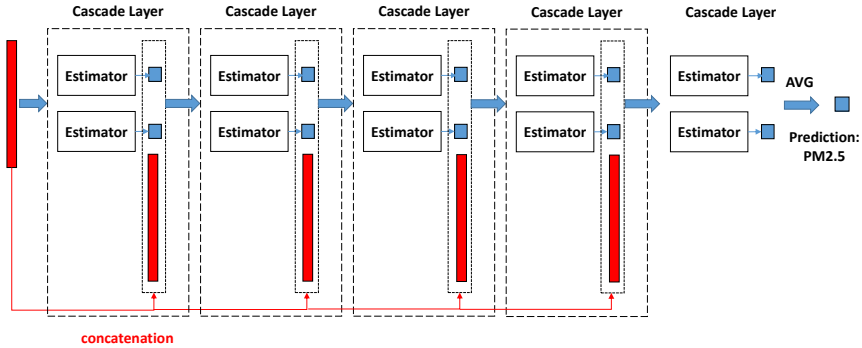


Fig. 2 Deep ensemble forest structure (with four cascade layers including two estimators per layer) for PM_{2.5} estimation

The modeling process formulated by the equation above is a regression problem, and machine learning techniques can be applied to examine different hypotheses that better describe the relationship between input features and the target variable (PM_{2.5}). As mentioned in Section 1, in the literature, different regression techniques based on decision tree ensemble approaches and deep neural networks have been applied [T. Li et al. \(2017\)](#); [Sun et al. \(2021\)](#). In this study, deep ensemble forest as a state-of-the-art machine learning technique is developed for PM_{2.5} estimation and the potential of the developed method is evaluated to identify the best hypothesis that can describe the function F mentioned in eq. 1.

3.1 Structure of Deep Ensemble Forest

Deep ensemble forest is a deep model (similar to a deep neural network structure) using an ensemble of decision tree forests without the need for backpropagation [Zhou and Feng \(2017\)](#). In this way, its performance is highly competitive with deep neural networks while possessing fewer parameters and being more applicable with less amount of data. Fig. 2 displays the structure of a deep ensemble forest regressor, which employs the cascade layers to generate a deep model. In each layer, estimators have the task of feature transformation and lead to developing new augmented features. In the following, the main modules constructing the structure of deep ensemble forest is explained in more detail.

3.1.1 Cascade Layers

Inspired by deep neural network structures that rely on layer-by-layer data processing and feature extraction, deep ensemble forest utilizes a cascade structure for representation learning. Each cascade layer receives features extracted by the preceding cascade layer and transforms the input features to generate new features that will be injected into the next layer. Each layer comprises n number decision tree ensemble estimators that perform regression using the input features and target value (PM_{2.5} level). Each estimator generates a new

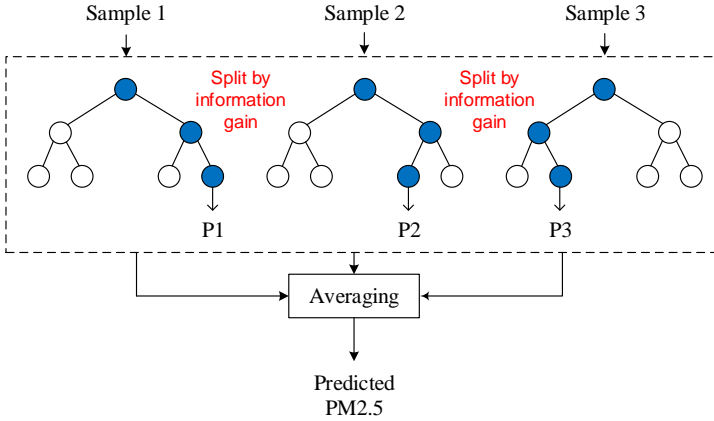


Fig. 3 Random Forest estimator for PM_{2.5} prediction

feature that will be input into the next cascade layer. Consequently, a new n -dimensional feature vector is achieved by n estimators. This feature vector is also called an augmented feature vector and can effectively realize the representation learning for the features of the sample. However, before that, the produced new features by estimators are concatenated with primary features inputted into the cascade layer (represented as a red chunk in Fig. 2). In other words, the new feature vector includes transformed features generated by estimators within the layer as well as initial input features [Zhou and Feng \(2017\)](#). Mathematically, let f^{inp} be the input feature vector, by using n estimators in a cascade layer j , the output feature vector can be formulated as below:

$$\begin{aligned} L_c^1 &= f^{inp} \cup_i^n R_i^1 \cup_i^n E_i^1 \\ L_c^j &= L_c^{j-1} \cup_i^n R_i^j \cup_i^n E_i^j, \end{aligned} \quad (2)$$

where L_c^j is the feature vector output from the j th cascade layer, R_i^j , and E_i^j are the output of random forest and extremely randomized trees estimators, respectively, embedded in the j^{th} layer, and \cup denotes the concatenation operator. Note that each decision tree in estimators randomly selects \sqrt{d} feature from L_c^{j-1} . The feature extraction and concatenation are continued until the last layer, in which the random forest and extremely randomized trees estimators predict the final outputs using feature values established by cascade layers. The outcome is an average of predictions achieved by estimators at the last layer.

3.1.2 Estimators

Two types of estimators, random forest regressor and extremely randomized trees formed based on the classification and regression tree (CART), can be

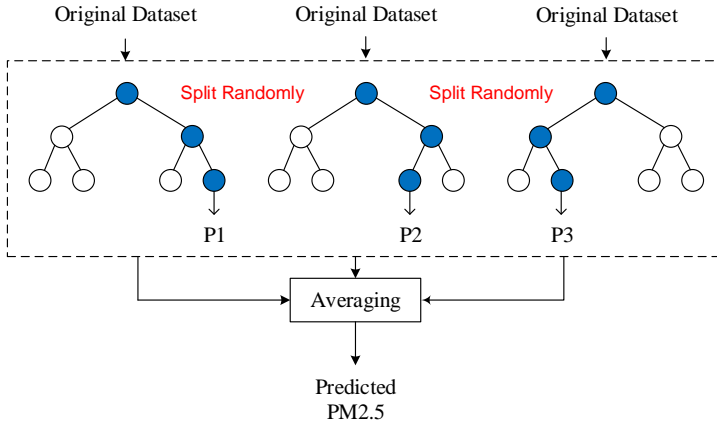


Fig. 4 Extra Trees estimator for PM_{2.5} prediction

employed at the heart of cascade layers to increase diversity as a crucial characteristic for ensemble learning. The estimators transform the input features to new augmented features, which will be concatenated with original features and be injected into the next layer.

As shown in Fig. 3, random forest as an ensemble method works based on fitting a decision tree on a bootstrapped dataset (samples) [James, Witten, Hastie, and Tibshirani \(2013\)](#). For this, a decision tree is built using a random subset of features. The split at each node is achieved by the optimal feature selected from the random subset using gain information. Building decision trees is repeated for m times by a new subset of features and a new bootstrapped dataset. Finally, the random forest model is formed based on the ensemble of m fitted decision tree regressors.

Extremely randomized trees (also called extra trees) is similar to random forest; However, in extra trees, one more randomization step has been added in the process of building decision trees [Geurts, Ernst, and Wehenkel \(2006\)](#). Instead of selecting the best feature for node split, the algorithm chooses the feature completely random from the subset at node split (Fig. 4). In this way, an extremely randomized trees estimator adds more diversity to the deep ensemble forest and are computationally more efficient than random forest estimators.

3.2 Comparative Study

In this study, the performance of the tuned deep ensemble forest for PM_{2.5} estimation was benchmarked in comparison with different machine learning algorithms. The simplest model can be established by using a simple linear regression technique, in which the AOD extracted at the location of the monitoring station is an input variable, and the ground PM_{2.5} measurement is an independent variable. The achieved linear equation is used for estimating PM_{2.5} in other locations. In addition to satellite retrieved AOD, meteorological data have shown their efficiency in estimating PM_{2.5} concentration as

auxiliary input features. In this situation, multivariate linear regression can be applied for the modeling.

Ensemble approaches combine decision trees as weak learners to generate more efficient predictors by diminishing defects of decision trees such as overfitting. The performance of algorithms such as random forest and extra trees which were explained earlier will also be assessed for AOD-PM_{2.5} modeling.

In recent years, deep neural networks have also been presented as an outperforming, state-of-the-art algorithm for many machine learning problems. The main characteristic of deep neural network is automatically feature extraction and engineering from raw input data such as images [Goodfellow, Bengio, Courville, and Bengio \(2016\)](#). Different types of deep neural networks have been developed for different problems. One type of deep neural network that can be developed for regression problems is deep autoencoder decoder (DAE) [Goodfellow et al. \(2016\)](#). In this type of network, an encoder extracts higher-level features from raw data. The network structure is restricted to a bottleneck at the midpoint of the model from which, the network attempts to reconstruct the input data. After fitting the model, the reconstruction part is discarded, and the model up to the bottleneck is applied for feature extraction. In the autoencoder part, input features are inputted into the network, and more higher-level learned features are generated through the network by the composition of lower-level features. This automatic feature extraction and engineering provide an opportunity to learn sophisticated function mapping between input features and target variables [T. Liu, Li, Yu, and Qin \(2017\)](#). In the PM_{2.5} concentration problem, the input features are injected into a DAE to generate more beneficial, higher-level features. Then the achieved features are injected into a regression method such as SVR to predict PM_{2.5} values observed at the monitoring stations, ultimately. This process is performed by training in which the network tries to extract more advanced features as well as their weights, participating in forming the regression model.

The deep belief network (DBN), which is made up of a stack of restricted Boltzmann machines (RBM), is another deep learning structure that can be used to estimate PM_{2.5}. Each RBM comprises two main layers: the visible layer as the input layer and the hidden layer. On the forward pass, activations are produced using the hidden units, and then, the features are reconstructed by visible units on the backward pass using fine-tuning. This process is performed in each RBM layer with an output of the previous layer [Hinton, Osindero, and Teh \(2006\)](#). The constructed features at the final RBM are converted into PM_{2.5} values.

4 Experimental Setup

4.1 Data Preparation for PM_{2.5} Estimation by Deep Ensemble Forest

The main objective of this paper is to apply the tuned deep ensemble forest for generating high resolution maps of PM_{2.5} using MAIAC AOD data.

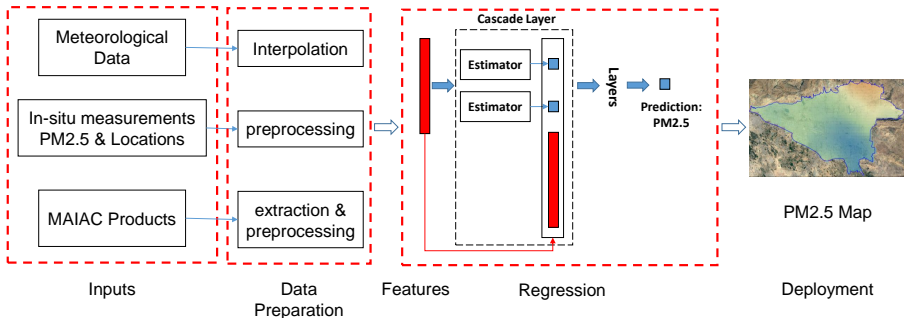


Fig. 5 The framework designed for estimation of PM_{2.5} over Tehran at 1 km resolution

Before developing any regression models such as deep ensemble forest and subsequently generating a high resolution PM_{2.5} map, it is required to prepare input features and corresponding target values (PM_{2.5}) in a structured (tabular) format. A framework that is appropriate for the study area is created for this purpose. The suggested framework is depicted in detail in Fig. 5. Data preprocessing, regression, and deployment are the three key modules of the framework. The data preprocessing includes several steps involving PM_{2.5} data preprocessing, AOD data extraction, and meteorological data preparation.

At first, PM_{2.5} data collected by AQCC of Tehran at air quality monitoring stations are preprocessed. After heating the ambient air to 50°C, TEOM measures PM_{2.5} values at stations, and the mass of dry PM is collected as measured PM_{2.5}. Consequently, the reported values should be modified according to the relation below Bagheri (2022):

$$PM_c = PM \left(1 - \frac{RH}{100}\right)^{-1}, \quad (3)$$

where PM_c is the modified level of observed PM at the ground station and RH is the relative humidity.

Daily PM_{2.5} values contain outliers that should be detected before usage. Outliers can simply be detected and subsequently removed by the interquartile range (IQR) Yang, Rahardja, and Fränti (2019). In this way, a PM_{2.5} observation that is between $Q_1 - IQR$ and $Q_3 + IQR$ is assumed an inlier. Note that Q_1 and Q_3 are the first and third quartiles of measured PM_{2.5}, respectively.

After PM_{2.5} data preparation, MAIAC AOD data should be normalized. This is realized using PBLH delivered by ECMWF model. The formulation for this normalization is as below Z. Wang, Chen, Tao, Zhang, and Su (2010):

$$nAOD = \frac{AOD}{PBLH}, \quad (4)$$

MAIAC AOD data are retrieved from observations collected by Aqua and Terra sensors on the MOIDS platform. Previous investigations have demonstrated that averaging of AODs provided by those sensors from observations of different orbital passes can be correlated with daily PM_{2.5} data Hu et al.

(2014); Lee, Liu, Coull, Schwartz, and Koutrakis (2011). However, the delivered MAIAC AOD retrievals can not be simply averaged to estimate PM_{2.5}. As shown in Fig. 5, to accurately estimate PM_{2.5} from MAIAC AOD data, several preprocessing steps should be performed on them. In more detail, a MAIAC AOD product involves different AOD retrievals achieved from observations of two Aqua and Terra sensors in several orbital passes. Thus, the first step of preprocessing is to average retrievals of each sensor separately to produce a daily AOD retrieval. The outputs will be a daily mean of AOD for Aqua (AOD_A) as well as a daily mean of AOD for Terra (AOD_T).

In addition, for the study area, a linear correlation between the AODs of two sensors with a coefficient of determination of 0.72 can be established. In this way, missing AOD values in each sensor can be estimated based on the available values in another sensor using linear regression. After filling in the missing values, the final AOD is achieved by merging the retrievals from both sensors (Aqua and Terra) by an averaging as below:

$$AOD = \frac{AOD_A + AOD_T}{2}. \quad (5)$$

After AOD data preparation, they are extracted at each location of the air quality station. For this purpose, a window with a size of 3×3 is applied at the location of each station to coincide with the corresponding MODIS pixel. The final AOD at the location is the mean of AOD values within the window.

In order to extract only high quality AODs, several criteria are considered. First, the output AOD from the window should be an average of at least three pixels that have valid values (non missing). Second, the standard deviation of AOD values within the window should be less than 0.5. This criterion prevents engaging severely fluctuated AOD values at the neighborhood in final computation (AOD averaging).

In parallel, the quality of AOD data is also extracted from the ‘‘Quality Assessment’’ (QA) file Lyapustin and Wang (2018). According to recommendations presented in the user guide of MAIAC data, AOD data are filtered based on the adjacency mask and cloud mask in QA. The AODs have a normal condition or are clear in the adjacency mask as well as those that have been flagged clear or possibly cloudy in the cloud mask are selected.

Filtering AODs by aforementioned conditions reduces the number of samples that can affect the accuracy of models, particularly deep neural networks. Instead of filtering, a new feature describing the uncertainty of AOD measurements can be defined as below:

$$U = \frac{N_b}{N}, \quad (6)$$

where, U denotes the AOD uncertainty, N_b denotes the number of pixels satisfies conditions mentioned above, and N is the total number of pixels in a window. In other words, U identifies AOD uncertainty as the probability of the existence of AODs with the best quality in a window.

In addition to AOD data, meteorological data are also employed as valuable features for estimating PM_{2.5}. As mentioned in Section 2.3, the meteorological

data derived from ECMWF model (ERA5) must be calculated at the position of a ground station. Thus, the value of each meteorological parameter was interpolated at the position of the ground station using the kriging approach. The settings for interpolation of each parameter, such as kriging type and semi-variogram type, were determined by a grid search strategy [Bagheri, Sadeghian, and Sadjadi \(2014\)](#).

After preparing data in a structured format, they can be inputted into the regression module but before that, it is needed to normalize input values. As shown in [Tab. 1](#), the input features have diverse scales that can influence the performance of regression. Consequently, a min-max normalization strategy was applied to scale values of all input features between 0 and 1 as below:

$$f^n = \frac{f^i - f_{min}}{f_{max} - f_{min}}, \quad (7)$$

where f^i is the input feature, f_{max} and f_{min} are minimum and maximum values of corresponding input feature, and f^n denotes the normalized version of input feature value.

After data preparation, a machine learning algorithm is tuned for estimating the PM_{2.5} from the selected input features. After tuning the algorithm using training data, the performance of the achieved model is evaluated by test data. The main focus of this study is to develop the deep ensemble forest algorithm for this regression task. Additionally, other regression techniques are also examined in comparison to deep ensemble forest for PM_{2.5} concentration estimation. More details of deep ensemble forest implementation and tuning and comparison with other regression models will be provided in [Section 4.2](#).

As will be shown in [Section 5](#), the developed deep ensemble forest algorithm will outperform other models, and as a result, it will be used for high resolution estimation of PM_{2.5} over the study area. In this phase, similar preprocessing procedures explained earlier are accomplished to prepare AOD measurements and meteorological data at locations (pixels) where PM_{2.5} has not been sensed by ground sensors. In the following, PM_{2.5} can be estimated at each pixel of MAIAC AOD products by using the fitted deep ensemble forest model. In other words, in the deployment step, most of the processes performed in preprocessing and regression modeling stages are fulfilled on target pixels. The output is a 1 km PM_{2.5} map that represents the variation of PM_{2.5} over the study area.

4.2 Deep Ensemble Forest Setup

Deep ensemble forest regression was set up by a set of samples including input variables and corresponding PM_{2.5} through the k-fold cross-validation. The k-fold cross-validation was applied for hyperparameter setting as well as mitigating overfitting. In general, as k increases, the amount of bias in the estimation decreases. However, increasing the amount of k requires more computational cost, particularly, in case, the data volume is large. As a rule of thumb, k is considered to be 5 or 10 in most cases [Anguita, Ghelardoni, Ghio,](#)

Oneto, and Ridella (2012). In this research, according to the amount of data and the available computing facilities (available RAM = 16 GB), k was configured as 5. From around 20k samples, 70% of data was employed for k -fold cross-validation. The main hyperparameters of deep ensemble forest were set up using a grid search strategy with 5-fold cross-validation. The grid search found that the optimal number of cascade layers should be 2, the number of estimators should be 4 (two extra trees and two random forests), and the number of trees in each estimator should be 2000. Each tree was expanded until all leaves have 1 sample and no constraint was considered for trees.

After training, the performance of the developed deep ensemble forest was evaluated by test data (30% percent of remaining data) using standard metrics such as root mean square error (RMSE), mean absolute error (MAE), coefficient of determination (R^2), and absolute percentage error (APE) formulated as below:

$$RMSE = \sqrt{\frac{\sum_{i=1}^n (y_i - y_i^p)^2}{n}}, \quad (8)$$

$$MAE = \frac{\sum_{i=1}^n |y_i - y_i^p|}{n}, \quad (9)$$

$$R^2 = \left[\frac{n \sum_{i=1}^n y_i y_i^p - \sum_{i=1}^n y_i \sum_{i=1}^n y_i^p}{\sqrt{\left[n \sum_{i=1}^n y_i^2 - \left(\sum_{i=1}^n y_i \right)^2 \right] \left[n \sum_{i=1}^n (y_i^p)^2 - \left(\sum_{i=1}^n y_i^p \right)^2 \right]}} \right]^2, \quad (10)$$

$$APE = \frac{\sum_{i=1}^n |y_i - y_i^p|}{\sum_{i=1}^n y_i}, \quad (11)$$

In equations above, y_i is in-situ PM_{2.5} measurement, y_i^p is predicted PM_{2.5} by the regression model, and n denotes the number of samples.

4.3 Setup Algorithms to Compare with Deep Ensemble Forest

In this study, the performance of the tuned deep ensemble forest for PM_{2.5} estimation was benchmarked in comparison with different machine learning algorithms such as multivariate regressor, random forest, and extremely randomized trees which were described in Section 3.2. Similar to the deep ensemble forest setup, hyperparameters of each algorithm were determined using grid search strategy with 5-fold cross-validation as: multivariate regressor (no hyperparameters); random forest (number of trees is 500, maximum depth is 10; maximum features is 0.5, minimum samples in a leaf is 1); extra trees (number of trees is 1000, maximum depth is 10, maximum features is 0.8, minimum samples in a leaf is 1). All aforementioned algorithms were implemented using scikit-learn library Buitinck et al. (2013) in Python.

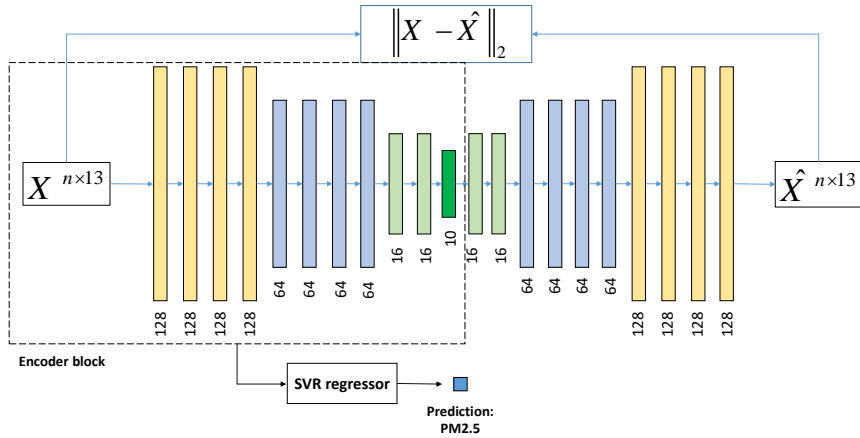


Fig. 6 The structure of deep autoencoder-decoder used for feature extraction. The SVR regressor applies the generated features for PM_{2.5} estimation.

In addition, two deep learning structures were implemented by the author in TensorFlow 2 to comparatively study the performance of deep ensemble forest. For this aim, a deep belief network (DBN) based on the restricted Boltzmann machine (RBM) was carried out. The optimal structure of the network was achieved by validation data. In this research, a DBN consisting of two RBM blocks, including one visible layer (input layer) and two hidden layers within 64, 10 neurons, was trained for PM_{2.5} estimation. Other hyperparameters were set to be: the learning rate of RBM is 0.01, the learning rate of the network is 0.001, the optimizer is stochastic gradient descent, number of epochs for training RBM is 50, number of backpropagation iteration is 200, mini-batch is 256, the activation function is ReLU, and loss is MSE.

The second experiment was accomplished by a support vector regressor (SVR) using features extracted from a deep autoencoder (DAE). For this, a deep autoencoder-decoder was employed to extract new transformed features. The structure of applied deep autoencoder-decoder is shown in Fig 6.

The number of neurons in each layer is expressed in the diagram of the network illustrated in Fig. 6. The features derived from the bottleneck layer (colored by dark green) are imported as input transformed variables into a SVR regressor. Other hyperparameters were set as: DAE (optimization is Adam, learning rate is 0.001, activation function is ReLU, loss function is MSE, regularization term is formed based on L_2 norm using weight penalty of 0.001, epoch is set 200, mini-batch size is 256) + SVR (kernel is chosen radial basis function, regularization parameter is 100, and epsilon is 0.1).

In all experiments, the same test dataset was employed for comparing results.

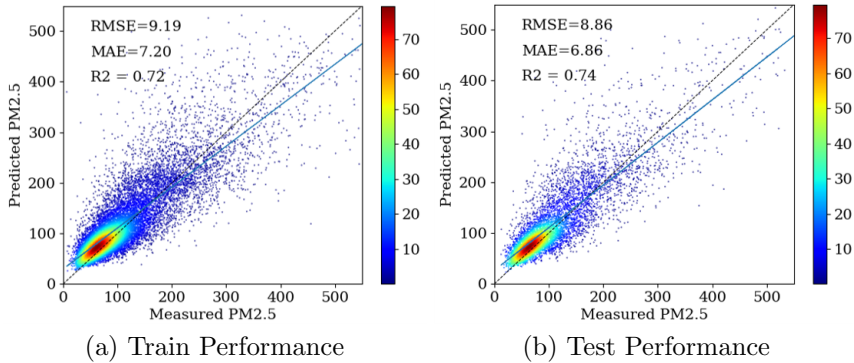


Fig. 7 Performance of the developed deep ensemble forest; a) on training data by k-fold cross-validation, and b) on test data

Table 2 The performances of deep ensemble forest in comparison to other machine learning models applied for PM_{2.5} estimation

Method	Model training: k-fold cross-validation				Model testing			
	RMSE $\frac{\mu g}{m^3}$	MAE $\frac{\mu g}{m^3}$	R^2	APE	RMSE $\frac{\mu g}{m^3}$	MAE $\frac{\mu g}{m^3}$	R^2	APE
Multivariate	13.45	10.42	0.54	36%	12.55	9.94	0.59	34%
Random Forest	9.81	7.83	0.68	27%	9.64	7.64	0.69	26%
Extra Trees	9.83	7.88	0.67	27%	9.77	7.79	0.68	27%
DBN	10.16	7.94	0.66	27%	9.69	7.40	0.68	26%
DAE + SVR	10.15	7.75	0.67	27%	9.94	7.47	0.67	26%
deep ensemble forest	9.19	7.20	0.72	25%	8.86	6.86	0.74	24%

5 Results and Discussion

5.1 Performance of Deep Ensemble Forest

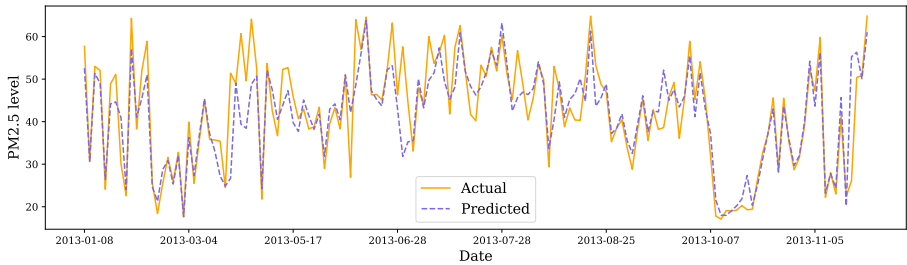
Fig. 7 illustrates the performance of the developed deep ensemble forest for building the PM_{2.5}-AOD relationship. The correlation plots are drawn for both training and test datasets. As shown in Fig. 7, the correlation between predicted PM_{2.5} and measured PM_{2.5} (at ground stations) is 0.72 and RMSE and MAE are 9.19 $\frac{\mu g}{m^3}$ and 7.20 $\frac{\mu g}{m^3}$, respectively. The results imply that the hyperparameter determination has been accomplished correctly by train data through the k-fold cross validation. However, it is required to evaluate the performance of the model with test data. In this regard, the performance of the algorithm was measured by test data. The correlation, RMSE, and MAE of the deep ensemble forest on test data were 0.74, 8.86 $\frac{\mu g}{m^3}$, 6.86 $\frac{\mu g}{m^3}$. It should be noted that the correlation plots were depicted based on scaled values of predicted PM_{2.5} (corrected PM_{2.5} i.e. PM_c , See eq. 3). However, the RMSE and MAE values were calculated after rescaling values to the initial scale.

Tab. 2 collects the performance of other machine learning techniques in comparison to the deep ensemble forest model on both training and test phases. This benchmarking gives a fair judgment of the ability of versatile machine learning techniques, deep learning, and deep ensemble forest for PM_{2.5} estimation. The comparison demonstrated that the deep ensemble forest was ranked

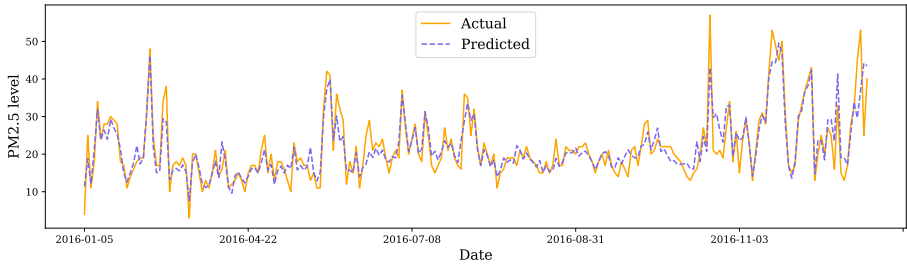
first in terms of performance measured by different metrics either on the train or test data. After that, based on MAE metric, the best results were obtained by DBN and DAE employing SVR as deep learning techniques owned to layer-by-layer processing and feature extraction by a deep structure, while the performance of DBN is slightly better than DAE. Compared to different traditional machine learning techniques, the highest performance was obtained by random forest as a decision tree ensemble approach. According to RMSE and R^2 , random forest also gives the highest accuracy among other comparative algorithms. The lowest accuracy was achieved by multivariate linear regression because of the simplicity of the method that could not model sophisticated patterns existing between input features and the output predictable variable (PM_{2.5}) properly.

In general, DBN, DAE+SVR algorithms, and random forest have almost similar performances based on different metrics (See Tab. 2). The main difference between three algorithms was represented by the MAE metric on both train and test data. The differences in MAE values are originated from the existing noise in input feature values. The AE structure reduced the noise effect own to its denoising property, while, the performance of random forest was more affected by noise that has led to slightly worse MAE.

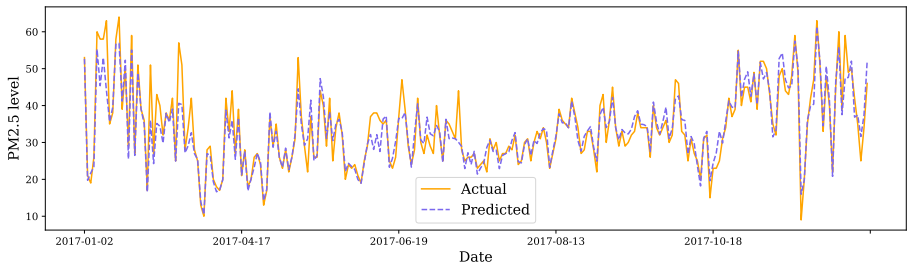
Fig. 8 visualizes times series of estimations of PM_{2.5} by the developed deep ensemble forest model at some exemplary air quality monitoring stations for different periods of study dates. At each geographical position, north-east; west; south; center, one station was selected as a sample to validate the accuracy of the tuned model for PM_{2.5} estimation. For comparison, time series of actual values were also depicted. Time series demonstrate that the deep ensemble forest model can estimate PM_{2.5} value correctly in most dates of observation. However, for some dates with peak values, the algorithm underestimates the level of PM_{2.5}. This underestimation is also illustrated by regression plots in Fig. 7. The estimation of PM_{2.5} by the deep ensemble forest model becomes lower than in-situ measurements for a higher level of concentration. In conclusion, as shown in Fig. 8, the deep ensemble forest can estimate PM_{2.5} in accordance with actual measurements in different dates and locations, generally.



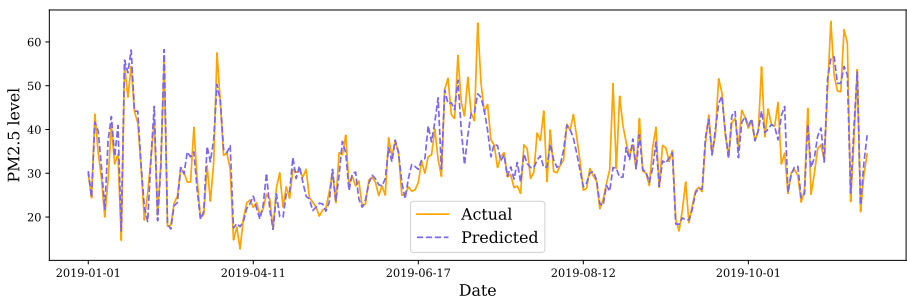
(a) Station Number: 1, Location: North-east of Tehran, Period: Jan. 2013 - Jan. 2014



(b) Station Number: 15, Location: South of city, Period: Jan. 2016 - Jan. 2017



(c) Station Number: 22, Location: Center of city, Period: Jan. 2017 - Jan. 2018



(d) Station Number: 7, Location: West of city, Period: Jan. 2019 - Jan. 2020

Fig. 8 Time series of PM_{2.5} estimation by the tuned deep ensemble forest at different exemplary stations in versatile locations and in different dates

From the achieved results, it can be concluded that deep learning techniques can exploit useful features through a deep model structure. Nevertheless, the strength of ensemble approaches in dealing with structured data such as PM_{2.5} estimation from AOD data has been proved in different investigations as mentioned in Section 1. Consequently, the deep ensemble forest algorithm by combining useful characteristics of deep learning and decision tree ensemble approaches such as layer-by-layer processing, feature transformation with a deep structure, and learning by the ensemble of ensembles could lead to better results while does not need any backpropagations for training.

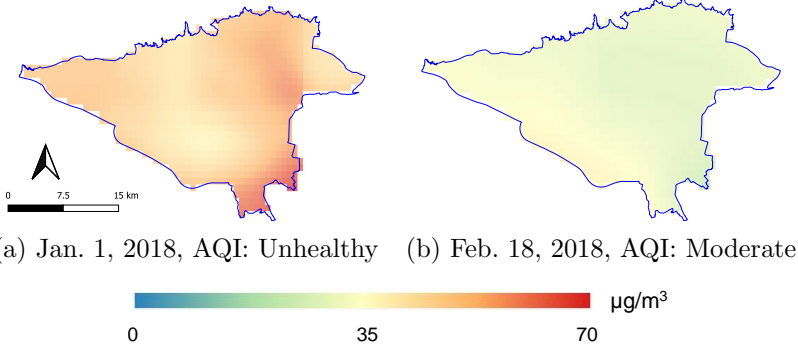
5.2 PM_{2.5} Concentration Mapping Using Deep Ensemble Forest

After developing the deep ensemble forest model, the tuned model was applied for high resolution (1 km) mapping of PM_{2.5} over the Tehran city. First, the daily PM_{2.5} map was produced using the input features (AODs from MAIAC, meteorological data, and others). Then, missing PM_{2.5} values were filled using kriging interpolation technique.

Fig. 9 displays the PM_{2.5} map of Tehran city in two days with different levels of PM_{2.5} concentration. One date (Jan. 1, 2018) is labeled as "Unhealthy" and another date (Feb. 18, 2018) is "Moderate" according to the report of AQCC of Tehran. As shown in Fig 9.a, predicted PM_{2.5} values by deep ensemble forest in most of the locations have a range between 35 and 70 $\frac{\mu g}{m^3}$. Statically, the maximum PM_{2.5} value predicted for the Jan. 1 is almost 69 $\frac{\mu g}{m^3}$. According to Tab. 3 which lists the air quality index based on the range of PM_{2.5}, the predicted PM_{2.5} values for Tehran at 1th of Jan. can be lay in "Unhealthy" category since most of the areas have a concentration of more than 55 $\frac{\mu g}{m^3}$ and less than 70 $\frac{\mu g}{m^3}$ (See map 9.a). On the 18th of Feb., the achieved map (Fig. 9.b) shows that most areas have PM_{2.5} concentration less than 35 $\frac{\mu g}{m^3}$. Thus, this date can be labeled as "Moderate" according to categories of air quality index (represented in Tab. 3) that is consistent with the report of AQCC. In conclusion, the developed deep ensemble forest can produce high resolution (1 km) PM_{2.5} map with sufficient accuracy that can predict the air quality index over the study area precisely.

Table 3 Categorization of air quality index based on the level of PM_{2.5}

PM _{2.5}	Air Quality Index
0 to 12.0	Good (0 to 50)
12.1 to 35.4	Moderate (51 to 100)
35.5 to 55.4	Unhealthy for Sensitive Groups (101 to 150)
55.5 to 150.4	Unhealthy (151 to 200)
150.5 to 250.4	Very Unhealthy (201 to 300)
250.5 to 500.4	Hazardous (301 to 500)

**Fig. 9** Daily, high resolution PM_{2.5} map of Tehran at a) Jan. 1, 2018 and b) Feb. 18, 2018.

The performance of deep ensemble forest was also verified by the annual estimation of PM_{2.5} concentration over the study area. In more detail, the yearly average of daily PM_{2.5} was led to an annual map of PM_{2.5}. Fig. 10 displays annual PM_{2.5} maps at 1 km realized by the deep ensemble forest model for years between 2013 and 2019. As shown by the annual PM_{2.5} maps, the concentration level of pollution alters between around $50 \frac{\mu\text{g}}{\text{m}^3}$ and $80 \frac{\mu\text{g}}{\text{m}^3}$. All generated maps through the deep ensemble forest deployment have almost similar patterns of pollution dispersion. In all maps, the pollution is concentrated in the northeast of Tehran. The results comply with the consequences of Atash (2007).

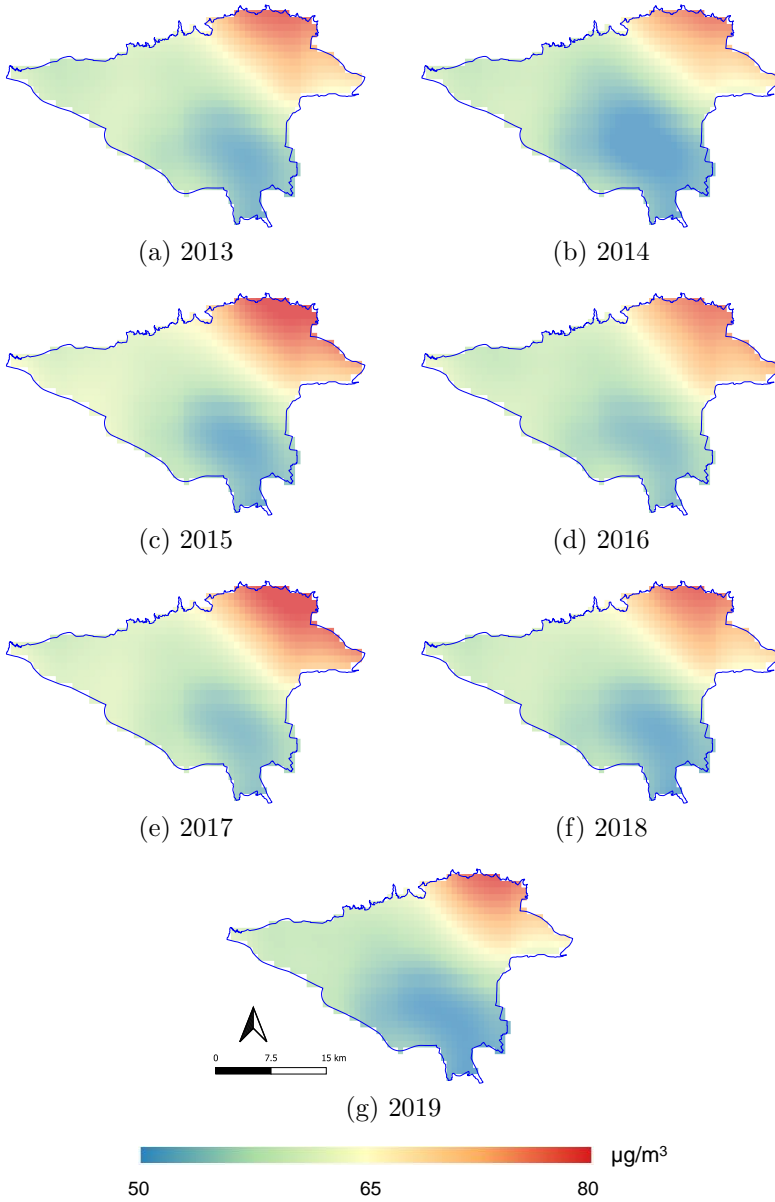


Fig. 10 Annual high resolution (1 km) maps of PM_{2.5} over Tehran city

For a better interpretation of generated maps, the corresponding annual wind maps, including directions and speeds of wind vectors as well as the topography map of the study area are depicted in Fig. 11 and 12, respectively.

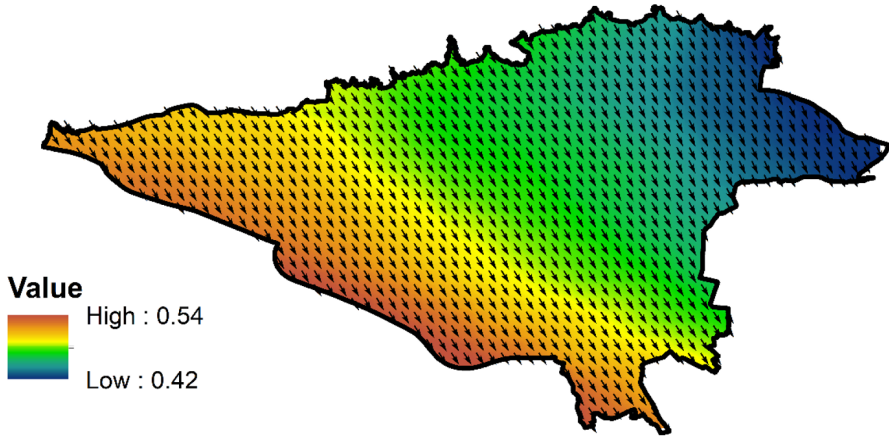


Fig. 11 Annual map of wind directions and speeds ($\frac{m}{s}$) over the study area in 2013

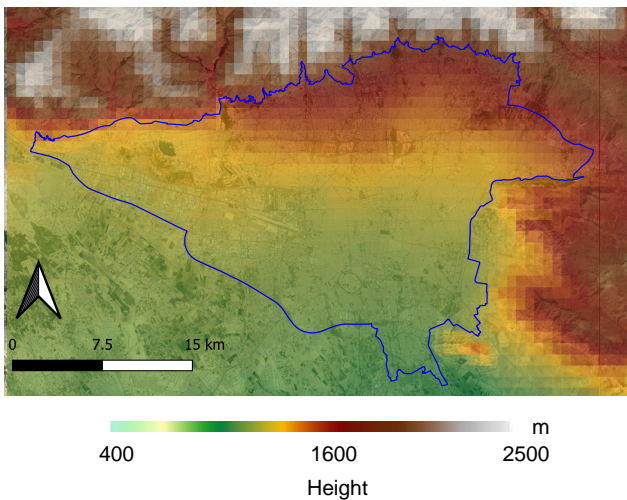


Fig. 12 Topography map of Tehran and surroundings.

As shown in wind map, all winds have almost the same direction from the northwest to the southeast. However, the wind speed decreases from the west to the east, where it reaches the minimum speed, 0.42 m/s . On the other hand, based on the topography representation, the east and the northeast are surrounded by the highest mountains. As a result, increasing the height of mountains as well as decreasing the wind speed in the east and the northeast of the city cause trapping pollutants and subsequently concentrating PM_{2.5} in this area more than other parts of the city.

6 Conclusion

This paper investigates the potential of deep ensemble forest for estimating PM_{2.5} concentration from satellite AOD data (MAIAC MODIS) and other parameters such as meteorological observations. The goal is to produce a high resolution (1 km) PM_{2.5} map in the study area, Tehran. For this, deep ensemble forest is developed to explore a regression function that will be used for PM_{2.5} estimation. The results of implemented experiments in this paper demonstrated the ability of deep ensemble forest in PM_{2.5} estimation. The algorithm was also compared with other machine learning techniques such as random forest, deep neural networks, etc. The comparison revealed that the developed deep ensemble forest could outperform other methods such as deep neural networks.

Acknowledgments

The author wishes to express his gratitude to everyone who contributed to this study, particularly Tehran's AQCC for the ground PM_{2.5} measurements, NASA for the MAIAC data, and ECMWF for the meteorological data.

Declarations

Ethical Approval

All authors have read, understood, and have complied as applicable with the statement on "Ethical responsibilities of Authors" as found in the Instructions for Authors and are aware that with minor exceptions, no changes can be made to authorship once the paper is submitted.

Conflict of Interest

The author declares that he has no conflict of interest.

Funding

This research received no specific grant from any funding agency in the public, commercial, or not-for-profit sectors.

Availability of data and materials

The data that support the findings of this study are available on request from the corresponding author.

References

- Ahmad, M., Alam, K., Tariq, S., Anwar, S., Nasir, J., Mansha, M. (2019). Estimating fine particulate concentration using a combined approach of linear regression and artificial neural network. *Atmospheric Environment*, 219, 117050.
- Anguita, D., Ghelardoni, L., Ghio, A., Oneto, L., Ridella, S. (2012). The ‘K’ in K-fold cross validation. *20th european symposium on artificial neural networks, computational intelligence and machine learning (esann)* (pp. 441–446).
- Arciszewska, C., & McClatchey, J. (2001). The importance of meteorological data for modelling air pollution using ADMS-Urban. *Meteorological Applications: A journal of forecasting, practical applications, training techniques and modelling*, 8(3), 345–350.
- Atash, F. (2007). The deterioration of urban environments in developing countries: Mitigating the air pollution crisis in Tehran, Iran. *Cities*, 24(6), 399-409.
- Bagheri, H. (2022). A machine learning-based framework for high resolution mapping of PM_{2.5} in Tehran, Iran, using MAIAC AOD data. *Advances in space Research*. (In press.)
- Bagheri, H., Sadeghian, S., Sadjadi, S.Y. (2014). The assessment of using an intelligent algorithm for the interpolation of elevation in the DTM generation. *Photogrammetrie - Fernerkundung - Geoinformation*, 2014(3), 197-208.
- Buitinck, L., Louppe, G., Blondel, M., Pedregosa, F., Mueller, A., Grisel, O., ... Varoquaux, G. (2013). API design for machine learning software: experiences from the scikit-learn project. *Ecml pkdd workshop: Languages for data mining and machine learning* (pp. 108–122).
- Chen, B., You, S., Ye, Y., Fu, Y., Ye, Z., Deng, J., ... Hong, Y. (2021). An interpretable self-adaptive deep neural network for estimating daily spatially-continuous PM_{2.5} concentrations across China. *Science of The Total Environment*, 768, 144724.

- Chen, W., Ran, H., Cao, X., Wang, J., Teng, D., Chen, J., Zheng, X. (2020). Estimating PM_{2.5} with high-resolution 1-km AOD data and an improved machine learning model over Shenzhen, China. *Science of The Total Environment*, 746, 141093.
- Di, Q., Kloog, I., Koutrakis, P., Lyapustin, A., Wang, Y., Schwartz, J. (2016). Assessing PM_{2.5} exposures with high spatiotemporal resolution across the continental United States. *Environmental science & technology*, 50(9), 4712–4721.
- ECMWF (2021). *ERA5*. <https://confluence.ecmwf.int/display/CKB/ERA5>. ([Accessed 02.21])
- Geurts, P., Ernst, D., Wehenkel, L. (2006). Extremely randomized trees. *Machine learning*, 63(1), 3–42.
- Ghotbi, S., Sotoudeheian, S., Arhami, M. (2016). Estimating urban ground-level PM₁₀ using MODIS 3km AOD product and meteorological parameters from WRF model. *Atmospheric Environment*, 141, 333–346.
- Goodfellow, I., Bengio, Y., Courville, A., Bengio, Y. (2016). *Deep learning* (Vol. 1) (No. 2). MIT press Cambridge.
- Gupta, P., & Christopher, S.A. (2009a). Particulate matter air quality assessment using integrated surface, satellite, and meteorological products: 2. A neural network approach. *Journal of Geophysical Research: Atmospheres*, 114(D20).
- Gupta, P., & Christopher, S.A. (2009b). Particulate matter air quality assessment using integrated surface, satellite, and meteorological products: Multiple regression approach. *Journal of Geophysical Research: Atmospheres*, 114(D14).
- Gupta, P., & Christopher, S.A. (2009c). Particulate matter air quality assessment using integrated surface, satellite, and meteorological products: Multiple regression approach. *Journal of Geophysical Research: Atmospheres*, 114(D14).
- Hersbach, H., Bell, B., Berrisford, P., Hirahara, S., Horányi, A., Muñoz-Sabater, J., ... Thépaut, J.-N. (2020). The ERA5 global reanalysis.

Quarterly Journal of the Royal Meteorological Society, 146(730), 1999–2049.

- Hinton, G.E., Osindero, S., Teh, Y.-W. (2006). A fast learning algorithm for deep belief nets. *Neural computation*, 18(7), 1527–1554.
- Hsu, N.C., Jeong, M.-J., Bettenhausen, C., Sayer, A.M., Hansell, R., Seftor, C.S., ... Tsay, S.-C. (2013). Enhanced deep blue aerosol retrieval algorithm: The second generation. *Journal of Geophysical Research: Atmospheres*, 118(16), 9296–9315.
- Hu, X., Waller, L.A., Lyapustin, A., Wang, Y., Al-Hamdan, M.Z., Crosson, W.L., ... others (2014). Estimating ground-level PM_{2.5} concentrations in the Southeastern United States using MAIAC AOD retrievals and a two-stage model. *Remote Sensing of Environment*, 140, 220–232.
- James, G., Witten, D., Hastie, T., Tibshirani, R. (2013). *An introduction to statistical learning* (Vol. 112). Springer.
- Klemm, R.J., Mason Jr, R.M., Heilig, C.M., Neas, L.M., Dockery, D.W. (2000). Is daily mortality associated specifically with fine particles? Data reconstruction and replication of analyses. *Journal of the Air & Waste Management Association*, 50(7), 1215–1222.
- Lee, H., Liu, Y., Coull, B., Schwartz, J., Koutrakis, P. (2011). A novel calibration approach of MODIS AOD data to predict PM_{2.5} concentrations. *Atmospheric Chemistry and Physics*, 11(15), 7991–8002.
- Li, L. (2020). A robust deep learning approach for spatiotemporal estimation of satellite aod and PM_{2.5}. *Remote Sensing*, 12(2).
- Li, T., Shen, H., Yuan, Q., Zhang, X., Zhang, L. (2017). Estimating ground-level PM_{2.5} by fusing satellite and station observations: A geo-intelligent deep learning approach. *Geophysical Research Letters*, 44(23), 11,985–11,993.
- Lin, C., Li, Y., Yuan, Z., Lau, A.K., Li, C., Fung, J.C. (2015). Using satellite remote sensing data to estimate the high-resolution distribution of ground-level PM_{2.5}. *Remote Sensing of Environment*, 156, 117–128.

- Lippmann, M., Ito, K., Nadas, A., Burnett, R. (2000). Association of particulate matter components with daily mortality and morbidity in urban populations. *Research Report (Health Effects Institute)*(95), 5–72.
- Liu, T., Li, Z., Yu, C., Qin, Y. (2017). NIRS feature extraction based on deep auto-encoder neural network. *Infrared Physics & Technology*, 87, 124–128.
- Liu, Y., Park, R.J., Jacob, D.J., Li, Q., Kilaru, V., Sarnat, J.A. (2004). Mapping annual mean ground-level PM_{2.5} concentrations using multiangle imaging spectroradiometer aerosol optical thickness over the contiguous United States. *Journal of Geophysical Research: Atmospheres*, 109(D22).
- Lyapustin, A., & Wang, Y. (2018). MODIS multi-angle implementation of atmospheric correction (MAIAC) data user’s guide. *NASA: Greenbelt, MD, USA*.
- Lyapustin, A., Wang, Y., Korkin, S., Huang, D. (2018). MODIS collection 6 MAIAC algorithm. *Atmospheric Measurement Techniques*, 11(10), 5741–5765.
- Lyapustin, A., Zhao, F., Wang, Y. (2021). A comparison of multi-angle implementation of atmospheric correction and MOD09 daily surface reflectance products from MODIS. *Frontiers in Remote Sensing*, 2.
- Ma, Z., Hu, X., Sayer, A.M., Levy, R., Zhang, Q., Xue, Y., . . . Liu, Y. (2016). Satellite-based spatiotemporal trends in PM_{2.5} concentrations: China, 2004–2013. *Environmental health perspectives*, 124(2), 184–192.
- Nabavi, S.O., Haimberger, L., Abbasi, E. (2019). Assessing PM_{2.5} concentrations in Tehran, Iran, from space using MAIAC, deep blue, and dark target AOD and machine learning algorithms. *Atmospheric Pollution Research*, 10(3), 889–903.
- Ni, X., Cao, C., Zhou, Y., Cui, X., P. Singh, R. (2018). Spatio-temporal pattern estimation of PM_{2.5} in Beijing-Tianjin-Hebei region based on

MODIS AOD and meteorological data using the back propagation neural network. *Atmosphere*, 9(3).

- Sayer, A., Hsu, N., Bettenhausen, C., Jeong, M.-J., Meister, G. (2015). Effect of MODIS Terra radiometric calibration improvements on collection 6 deep blue aerosol products: Validation and Terra/Aqua consistency. *Journal of Geophysical Research: Atmospheres*, 120(23), 12–157.
- Song, W., Jia, H., Huang, J., Zhang, Y. (2014). A satellite-based geographically weighted regression model for regional PM_{2.5} estimation over the Pearl River Delta region in China. *Remote Sensing of Environment*, 154, 1–7.
- Sotoudeheian, S., & Arhami, M. (2014). Estimating ground-level PM₁₀ using satellite remote sensing and ground-based meteorological measurements over Tehran. *Journal of Environmental Health Science and Engineering*, 12(1), 1–13.
- Sun, J., Gong, J., Zhou, J. (2021). Estimating hourly PM_{2.5} concentrations in Beijing with satellite aerosol optical depth and a random forest approach. *Science of The Total Environment*, 762, 144502.
- Van Donkelaar, A., Martin, R.V., Brauer, M., Kahn, R., Levy, R., Verduzco, C., Villeneuve, P.J. (2010). Global estimates of ambient fine particulate matter concentrations from satellite-based aerosol optical depth: development and application. *Environmental health perspectives*, 118(6), 847–855.
- Wang, J., & Christopher, S.A. (2003a). Intercomparison between satellite-derived aerosol optical thickness and PM_{2.5} mass: Implications for air quality studies. *Geophysical Research Letters*, 30(21).
- Wang, J., & Christopher, S.A. (2003b). Intercomparison between satellite-derived aerosol optical thickness and PM_{2.5} mass: Implications for air quality studies. *Geophysical Research Letters*, 30(21).
- Wang, X., & Sun, W. (2019). Meteorological parameters and gaseous pollutant concentrations as predictors of daily continuous PM_{2.5} concentrations using deep neural network in Beijing–Tianjin–Hebei, China. *Atmospheric Environment*, 211, 128–137.

- Wang, Z., Chen, L., Tao, J., Zhang, Y., Su, L. (2010). Satellite-based estimation of regional particulate matter (PM) in Beijing using vertical-and-RH correcting method. *Remote sensing of environment*, 114(1), 50–63.
- Weizhen, H., Zhengqiang, L., Yuhuan, Z., Hua, X., Ying, Z., Kaitao, L., ... Yan, M. (2014). Using support vector regression to predict PM₁₀ and PM_{2.5}. *IOP Conference Series: Earth and Environmental Science*, 17, 012268.
- Xiao, Q., Wang, Y., Chang, H.H., Meng, X., Geng, G., Lyapustin, A., Liu, Y. (2017). Full-coverage high-resolution daily PM_{2.5} estimation using MAIAC AOD in the Yangtze river delta of China. *Remote Sensing of Environment*, 199, 437–446.
- Yang, J., Rahardja, S., Fränti, P. (2019). Outlier detection: how to threshold outlier scores? *Proceedings of the international conference on artificial intelligence, information processing and cloud computing* (pp. 1–6).
- Yao, F., Si, M., Li, W., Wu, J. (2018). A multidimensional comparison between MODIS and VIIRS AOD in estimating ground-level PM_{2.5} concentrations over a heavily polluted region in China. *Science of The Total Environment*, 618, 819–828.
- You, W., Zang, Z., Pan, X., Zhang, L., Chen, D. (2015). Estimating PM_{2.5} in Xi'an, China using aerosol optical depth: A comparison between the MODIS and MISR retrieval models. *Science of The Total Environment*, 505, 1156–1165.
- Zamani Joharestani, M., Cao, C., Ni, X., Bashir, B., Talebiesfandarani, S. (2019). PM_{2.5} prediction based on random forest, XGBoost, and deep learning using multisource remote sensing data. *Atmosphere*, 10(7).
- Zhou, Z.-H., & Feng, J. (2017). Deep forest: Towards an alternative to deep neural networks. *Proceedings of the twenty-sixth international joint conference on artificial intelligence, IJCAI-17* (pp. 3553–3559).